ELECTROMAGNETIC SCATTERING FROM TWO DIMENSIONAL ANISOTROPIC IMPEDANCE OBJECTS UNDER OBLIQUE PLANE WAVE INCIDENCE

Ahmed A. Kishk and Per-Simon Kildal*

Department of Electrical Engineering
University of Mississippi, University, MS 38677, USA
*Department of Microwave Technology
Chalmers University of Technology, S-412 96 Gothenburg, Sweden

ABSTRACT. The surface integral equations of a two dimensional (2D) anisotropic impedance object is formulated to obtain the electromagnetic scattered fields due to oblique plane wave incidence. The surface impedance is anisotropic with arbitrary principle directions. The moment method with pulse basis functions and point matching is used to reduce the surface integral equations to a matrix equation. Four different formulations are generated for the problem. The surface current distributions and the scattered far fields are verified against the analytical series solutions of circular impedance cylinders. Very good agreement between the numerical and the analytical solutions is obtained. A rectangular cylinder made of four soft surfaces is analyzed for oblique incidence to verify that the results behave as expected. The computer code is also verified by comparing the solutions of the different formulations against each other.

1 INTRODUCTION

Some complicated structures can be modeled approximately using the concept of surface impedance, such as e.g. corrugated objects or objects coated with lossy material or thin dielectric layers, which can even be loaded with metal strips. The surface impedance model deals with the outer boundary of the structure in terms of an equivalent surface impedance, which can be obtained from the expected local relation between the tangential components of the electric and magnetic fields on the outer boundary. This relation can be found approximately at any surface point from the solution of a canonical problem which is similar to the local geometry around this point. The equivalent surface impedance is generally anisotropic, even if the coating is isotropic, in particular at an outer surface that has two different principle curvatures. Also, structures with periodic surface discontinuities such as corrugations or strip loaded coatings can be modeled using the anisotropic surface impedance concept, if the periods of the corrugations or strips are smaller than half the wavelength. The advantage with the surface impedance concept is that the numerical analysis of the object becomes simpler and takes shorter time. This is because the exact geometry of the loads do not need to be modelled so the problem description becomes easier and the number of unknowns can be significantly reduced.

The impedance boundary conditions (IBC) is a valid approximation under certain conditions [1], more references on the IBC can be found in [2]. The use of the IBC can simplify the analysis of some classes of complex electromagnetic problems, but it must be used with care as it may sometimes give erroneous results [3]. In order to widen the applicability of the IBC, generalized impedance boundary conditions (GIBC) was proposed in [4] and later improved for coated 2D structures [5] at the expense, however, of considerable analytical complications which requires specialized researchers to work with such problems. So far, the GIBC has only been used in connection with coated metallic surfaces without corrugations. On the other hand, the IBC has been used successfully to analyze corrugated horns and waveguides [6].

Anisotropic surface impedances have also been used to define soft and hard surfaces [7] that theoretically provides polarization independent soft and hard boundary conditions for electromagnetic waves of known propagation direction. The concept of soft and hard surfaces is also a way of thinking that can help to generate ideas for improved electromagnetic designs. Analysis tools based on the IBC are very important also to verify such thought models initially before the accurate analysis including all surface details is performed for the final design optimization. An example of how to use the concept of soft and hard surfaces to reduce the forward scattering from two dimensional (2D) structures is described in [8].

Previous papers have formulated the problem of electro-

This work was performed while Professor Kishk was on sabbatical leave at Chalmers University of Technology.

magnetic scattering from 2D impedance structures due to a normally incident plane wave [9-10]. Oblique incidence is considered in [11-12] for the case of an isotropic surface impedance. In [11], the finite element method is used for an arbitrary cross-section, and in [12] the finite difference method in the frequency domain is used for elliptic cross-sections. In [13] the method of moment is used for bodies of revolution with anisotropic surface impedance. In the present paper the problem of scattering from a two dimensional object of arbitrary cross-section and anisotropic surface impedance is formulated for oblique plane wave incidence.

The present formulation is based on the surface integral equation and solved using the method of moment with pulse basis functions and point matching. With the proper implementation of this simple expansion and testing, accurate numerical solutions are obtained. The numerical solution is verified with the exact solution of a circular cylinder [14]. Different surface integral formulations are generated and found useful in the verification of the numerical solutions for arbitrary objects. In addition a theoretical example is constructed for which the E-field solution for TM_z incidence should be equal to the H-field solution for TE_z incidence. The example is a 2D object with rectangular cross section made of four surfaces which are soft as defined in [7] for the given oblique incidence. Finally, it should be mentioned that the formulations in the present paper describe what in [15] is referred to as a harmonic 2D solutions, and that these can be extended to an arbitrary incident field, i.e. three dimensional sources, by considering a spectrum of 2D solutions [15].

2 IMPEDANCE BOUNDARY CONDITION

The impedance boundary condition (IBC) for exterior fields E_0 and H_0 at a surface S with surface normal $\hat{u}_n$ can generally be stated in vector form as

$$E_0 - (E_0 \cdot \hat{u}_n)\,\hat{u}_n = \eta_0 \overleftrightarrow{\eta} \cdot (\hat{u}_n \times H_0) \tag{1}$$

where η_0 is the free space intrinsic impedance and

$$\overleftrightarrow{\eta} = \eta_{\zeta\zeta}\,\hat{u}_\zeta \hat{u}_\zeta + \eta_{\zeta\xi}\,\hat{u}_\zeta \hat{u}_\xi + \eta_{\xi\zeta}\,\hat{u}_\xi \hat{u}_\zeta + \eta_{\xi\xi}\,\hat{u}_\xi \hat{u}_\xi \tag{2}$$

is the anisotropic surface impedance dyad, given in terms of its components in a local surface coordinate system defined by the unit vectors $\hat{u}_\zeta$, $\hat{u}_\xi$ and $\hat{u}_n$ with $\hat{u}_\zeta \perp \hat{u}_\xi$ and $\hat{u}_n = \hat{u}_\xi \times \hat{u}_\zeta$. We can also express this in a matrix form as

$$\begin{bmatrix} E_\zeta \\ E_\xi \end{bmatrix} = \eta_0 \, [\eta] \begin{bmatrix} H_\xi \\ -H_\zeta \end{bmatrix} \tag{3}$$

with

$$[\eta] = \begin{bmatrix} \eta_{\zeta\zeta} & \eta_{\zeta\xi} \\ \eta_{\xi\zeta} & \eta_{\xi\xi} \end{bmatrix} \tag{4}$$

where E_ζ, E_ξ (H_ζ, H_ξ) are the components of the E-field (H-field) along $\hat{u}_\zeta$ and $\hat{u}_\xi$, respectively. The IBC is based on the fact that we in some cases know exactly or approximately the field solution inside the surface, and that this solution is the same or approximately the same for all excitations (incidences) considered. The inner field solution can then be characterized by the relations between its E- and H-fields at the surface, i.e. the surface impedances $\eta_{\zeta\zeta}$, $\eta_{\zeta\xi}$, $\eta_{\xi\zeta}$ and $\eta_{\xi\xi}$. The IBC applied to the exterior fields thereby means that the continuity of the E- and H-fields are enforced over the surface S (when the form of the inner field solution is given).

When the surface impedance is anisotropic, we can normally find two principle directions $\hat{u}_\xi$ and $\hat{u}_\zeta$ which make $\overleftrightarrow{\eta}$ diagonal, according to

$$\overleftrightarrow{\eta} = \eta_{\zeta\zeta}\,\hat{u}_\zeta \hat{u}_\zeta + \eta_{\xi\xi}\,\hat{u}_\xi \hat{u}_\xi \tag{5}$$

From now on we will let $\hat{u}_\xi$ and $\hat{u}_\zeta$ denote these principle directions of $\overleftrightarrow{\eta}$. The following example will explain how $\hat{u}_\xi$ and $\hat{u}_\zeta$ are related to the surface structure. Let us assume a corrugated surface with the corrugations parallel with $\hat{u}_\xi$. Then, the $\hat{u}_\xi$ component of the E-field will be shorted by the thin ridges between the corrugations, so that $\eta_{\xi\xi} = 0$, and the $\hat{u}_\zeta$ component E_ζ of the E-field will couple to a TE to $\hat{u}_n$ mode in each corrugation, which acts as a shorted parallel plate waveguide if the corrugation are straight. The E_ζ inside the parallel plate waveguide is related to H_ξ according to (see e.g. [7])

$$\eta_0 \eta_{\zeta\zeta} = -\frac{E_\zeta}{H_\xi} = -j\,\eta_c \tan(k_n d) \tag{6}$$

where k_n is the component of the wave number in the $\hat{u}_n$ direction inside the corrugations, d is the corrugation depth, and η_c is the intrinsic impedance inside the corrugation. This assumption is good when k_n is known and independent of the angle of incidence. This is the case for corrugations that are transverse to the direction of incidence of the wave.

We can transform $\overleftrightarrow{\eta}$ in (5) to any coordinate system defined by vectors $\hat{u}_\tau \perp \hat{u}_n$ and $\hat{u}_z = \hat{u}_n \times \hat{u}_\tau$ according to

$$\overleftrightarrow{\eta} = \eta_{zz}\,\hat{u}_z\hat{u}_z + \eta_{z\tau}\,\hat{u}_z\hat{u}_\tau + \eta_{\tau z}\,\hat{u}_\tau\hat{u}_z + \eta_{\tau\tau}\,\hat{u}_\tau\hat{u}_\tau \tag{7}$$

where

$$\begin{aligned}
\eta_{zz} &= \eta_{\zeta\zeta}(\hat{u}_\zeta \cdot \hat{u}_z)(\hat{u}_\xi \cdot \hat{u}_\tau) - \eta_{\xi\xi}(\hat{u}_\xi \cdot \hat{u}_z)(\hat{u}_\zeta \cdot \hat{u}_\tau) \\
\eta_{\tau z} &= \eta_{\zeta\zeta} - \eta_{\xi\xi})(\hat{u}_\zeta \cdot \hat{u}_z)(\hat{u}_\xi \cdot \hat{u}_z) \\
\eta_{z\tau} &= (\eta_{\zeta\zeta} - \eta_{\xi\xi})(\hat{u}_\zeta \cdot \hat{u}_\tau)(\hat{u}_\xi \cdot \hat{u}_\tau) \\
\eta_{\tau\tau} &= \eta_{\zeta\zeta}(\hat{u}_\xi \cdot \hat{u}_z)(\hat{u}_\zeta \cdot \hat{u}_\tau) - \eta_{\xi\xi}(\hat{u}_\zeta \cdot \hat{u}_z)(\hat{u}_\xi \cdot \hat{u}_\tau)
\end{aligned} \tag{8}$$

3 FORMULATION

Consider a two dimensional (2D) anisotropic impedance scatterer of infinite extent in the z-direction and with arbitrary cross section (Fig. 1). For this geometry, there are two distinct regions V_1 and V_0, where V_1 constitutes the impedance body which is bounded by the surface S and V_0 is the unbounded region outside S. The surface S is described by the contour C in the xy-plane and has an outward surface normal $\hat{u}_n$ which is orthognal to $\hat{u}_z$. The surface is characterized by the anisotropic surface impedance dyad $\overleftrightarrow{\eta}$, as defined in the previous section, where $\eta_{\zeta\zeta}$, $\eta_{\xi\xi}$, $\hat{u}_\zeta$ and $\hat{u}_\xi$ are allowed to vary around C.

V_0 is the exterior region characterized by the permittivity and permeability of the free space (ϵ_0, μ_0). The total electric and magnetic fields in region V_0 are denoted by E_0 and H_0, respectively. The excitation is assumed to be an obliquely incident plane wave propagating in th-e direction

$$\begin{aligned}
\hat{k} = -\hat{u}_r(\theta_{inc}, \phi_{inc}) &= -\cos\phi_{inc}\sin\theta_{inc}\,\hat{u}_x \\
&- \sin\phi_{inc}\sin\theta_{inc}\,\hat{u}_y - \cos\theta_{inc}\,\hat{u}_z
\end{aligned} \tag{9}$$

making an angle θ_{inc} with the z-axis and ϕ_{inc} measured from

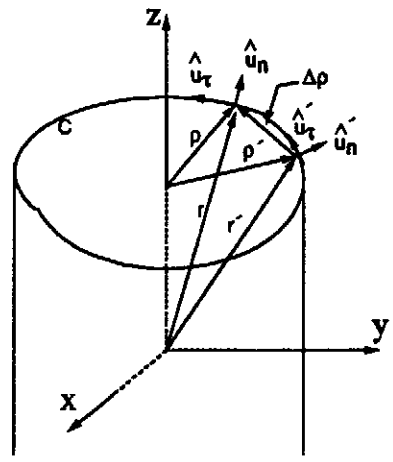

Fig. 1 Geometry of the original problem.

the x-axis in the xy-plane. The incident field at a point r is therefore described by

$$E^{inc} = E_m(E^p\cos\alpha_{inc} + E^n\sin\alpha_{inc})\,e^{-jk_0\hat{k}\cdot r} \tag{10}$$

$$H^{inc} = (\hat{k} \times E^{inc})/\eta_0 \tag{11}$$

where

$$r = x\,\hat{u}_x + y\,\hat{u}_y + z\,\hat{u}_z = \rho + z\,\hat{u}_z \tag{12}$$

$$\begin{aligned}
E^p = -\hat{u}_\theta(\theta_{inc}, \phi_{inc}) &= -\hat{u}_x\cos\theta_{inc}\cos\phi_{inc} \\
&- \hat{u}_y\cos\theta_{inc}\sin\phi_{inc} + \hat{u}_z\sin\theta_{inc}
\end{aligned} \tag{13}$$

$$E^n = -u_\phi(\phi) = \hat{u}_x\sin\phi_{inc} - \hat{u}_y\cos\phi_{inc} \tag{14}$$

E^p and E^n are the unit vectors corresponding to polarizations parallel (TM_z case) and normal (TE_z) to the plane defined by the z-axis and $\hat{k}$. The polarization angle α_{inc} is the angle the incident electric field makes with the plane of incidence. If $\alpha_{inc}=0$, the plane wave is TM_z polarized (θ-polarized), and if $\alpha_{inc}=\pi/2$ the plane wave is TE_z polarized (ϕ-polarized). k_0 is the wave number in the free space, $\hat{u}_x$, $\hat{u}_y$ and $\hat{u}_z$ are the unit vectors in the direction of x, y, and z, respectively and $\hat{u}_r(\theta_{inc}, \phi_{inc})$, $\hat{u}_\theta(\theta_{inc}, \phi_{inc})$, and $\hat{u}_\phi(\phi_{inc})$ are the unit vectors in the direction of r, θ_{inc}, and ϕ_{inc} in the spherical coordinate system. The complex constant E_m is the amplitude of the plane wave.

Using the equivalence principle the object can be replaced by the material of the region V_0 and the equivalent electric surface current J and the equivalent magnetic surface current M on the surface, which produce zero fields in the region V_1 and $(E_0\text{-}E^{inc})$ and $(H_0\text{-}H^{inc})$ in the region V_0, where

$$J = \hat{u}_n \times H_0 \quad and \quad M = E_0 \times \hat{u}_n \quad on \quad S \tag{15}$$

For infinite cylindrical structures the electric and magnetic currents are assumed to be of the form

$$J(r') = J(\rho')\, e^{jk_z z} \tag{16}$$

and correspondingly for M, where $k_z = k\cos\theta_{inc}$. These assumptions are evident for isotropic surface boundaries as explained in [15], and we see no reason why it should not apply to anisotropic impedance surfaces as well. The magnetic and electric vector potentials, A and F, due to the equivalent currents J and M can be written as

$$\begin{Bmatrix} A(r) \\ F(r) \end{Bmatrix} = \begin{Bmatrix} \mu_0 \\ \epsilon_0 \end{Bmatrix} \int_{-\infty}^{\infty} \int_c G(r,r') \begin{Bmatrix} J(r') \\ M(r') \end{Bmatrix} dr'\, dz' \tag{17}$$

where $G(r, r')$ is the three-dimensional free space Green's function and dr' is the integration increment along the contour C in the cross-sectional plane. The three-dimensional Green's function can be written as

$$G(r,r') = \frac{e^{-jk(|\rho-\rho'|^2 + (z-z')^2)^{1/2}}}{(|\rho-\rho'|^2 + (z-z')^2)^{1/2}} \tag{18}$$

where r and r' are the position vectors of the observation and source points, respectively. ρ and ρ' are the cylindrical vector coordinates of the field and source points, respectively. After performing the known z integral we get

$$\begin{Bmatrix} A(r) \\ F(r) \end{Bmatrix} = \frac{e^{jk_z z}}{4j} \begin{Bmatrix} \mu_0 \\ \epsilon_0 \end{Bmatrix} \int_c H_0^{(2)}(k_\rho\, |\, \rho-\rho'\, |) \begin{Bmatrix} J(\rho') \\ M(\rho') \end{Bmatrix} dr' \tag{19}$$

where $k_\rho = \sqrt{k^2 - k_z^2}$, $k_z = -k\cos\theta_i$, and $H_0^{(2)}(\,)$ is the Hankel function of zeroth order and second type. This indicates that the magnetic vector potential of the three dimensional form is the same as the two dimensional form multiplied by $\exp(jk_z z)$ [15]. Both $J(\rho')$ and $M(\rho)$ have components both in the longitudinal $\hat{u}_z$ direction and in the transverse $\hat{u}_\tau$ direction, i.e.

$$\begin{Bmatrix} J \\ M \end{Bmatrix} = \begin{Bmatrix} J_z \\ M_z \end{Bmatrix} \hat{u}_z + \begin{Bmatrix} J_\tau \\ M_\tau \end{Bmatrix} \hat{u}_\tau \qquad on\ S, \tag{20}$$

where the transverse unit tangent is defined by

$$\hat{u}_\tau = \hat{u}_z \times \hat{u}_n \tag{21}$$

where $\hat{u}_n$ is the unit normal to S.

We can now obtain the electric and magnetic fields $E(\rho)$ and $H(\rho)$ due to the electric current $J(\rho')$ by using

$$H(r) = \frac{1}{\mu_0} \nabla \times A(r) \quad and \quad E(r) = -\frac{j}{\omega \epsilon_0} \nabla \times H(r) \tag{22}$$

where the ∇ operator in our case can be expressed as

$$\nabla = \nabla_\tau \hat{u}_\tau - jk_z \hat{u}_z \quad and \quad \nabla_\tau = \frac{\partial}{\partial x}\hat{u}_x + \frac{\partial}{\partial y}\hat{u}_y. \tag{23}$$

After some mathematical manipulations the electric and magnetic fields due to the electric currents can be expressed in operator form as shown in Appendix A. Expressions are given for $E_{zz}(J_z)$ $E_{\tau z}(J_z)$, $E_{z\tau}(J_\tau)$, and $E_{\tau\tau}(J_\tau)$ which are each of the components of the vector operator $E_{tan}(J)$ for the tangential E-field at a point ρ on S, and similarly for the tangential H-field vector operator $H_{tan}(J)$, i.e.

$$\begin{aligned} E_{tan}(J) &= [E_{zz}(J_z) + E_{z\tau}(J_\tau)]\hat{u}_z + [E_{\tau z}(J_z) + E_{\tau\tau}(J_\tau)]\hat{u}_\tau \\ H_{tan}(J) &= [H_{zz}(J_z) + H_{z\tau}(J_\tau)]\hat{u}_z + [H_{\tau z}(J_z) + H_{\tau\tau}(J_\tau)]\hat{u}_\tau \end{aligned} \tag{24}$$

The fields due to the magnetic current $M(\rho')$ can be obtained using duality (ch. 3, sec. 3-2 [16]).

We will now apply the impedance boundary condition in Eq. (1) to the field at S. The result is an integral equation

in terms of the unknown electric and magnetic currents of the form

$$-\frac{1}{\eta_0}E_{\tan}(J)-\frac{1}{\eta_0}E_{\tan}(M)+\overleftrightarrow{\eta}\cdot(\hat{u}_n\times\{H_{\tan}(J)+H_{\tan}(M)\})=\frac{1}{\eta_0}E^{inc}_{\tan}-\overleftrightarrow{\eta}\cdot(\hat{u}_n\times H^{inc}_{\tan}) \qquad on\ S \tag{25}$$

We will now use (1) to express M_z and M_τ in terms of J_z and J_τ, as follows. We cross multiply both sides of (1) with $\hat{u}_n$ and use (15) to obtain

$$M = \eta_0(\overleftrightarrow{\eta}\cdot J)\times\hat{u}_n \tag{26}$$

We substitute (20) for J and multiply both sides with $\hat{u}_z$ and $\hat{u}_\tau$ to get

$$\begin{aligned} M_z &= M\cdot\hat{u}_z=\eta_0[\overleftrightarrow{\eta}\cdot(J_z\hat{u}_z+J_\tau\hat{u}_\tau)]\times\hat{u}_n]\cdot\hat{u}_z \\ &= -\eta_0(\eta_{\tau\tau}J_\tau+\eta_{\tau z}J_z) \\ M_\tau &= M\cdot\hat{u}_\tau=\eta_0[\overleftrightarrow{\eta}\cdot(J_z\hat{u}_z+J_\tau\hat{u}_\tau)]\times\hat{u}_n]\cdot\hat{u}_\tau \\ &= \eta_0(\eta_{z\tau}J_\tau+\eta_{zz}J_z) \end{aligned} \tag{27}$$

respectively, with η_{zz}, $\eta_{z\tau}$, $\eta_{\tau z}$ and $\eta_{\tau\tau}$ defined in (8). By inserting (27) in (24) and (24) in (25) we get the final integral equation

$$\begin{aligned} &-\frac{1}{\eta_0}[E_{zz}(J_z)+E_{z\tau}(J_\tau)+E_{z\tau}(M_\tau)]+\eta_{zz}[H_{\tau z}(J_z)+H_{\tau\tau}(J_\tau)+H_{\tau z}(M_z)+H_{\tau\tau}(M_\tau)]-\eta_{z\tau}[H_{z\tau}(J_\tau)+ \\ &H_{zz}(M_z)+H_{z\tau}(M_\tau)]=\frac{1}{\eta_0}(E^{inc}_z-\eta_{zz}H^{inc}_\tau+\eta_{z\tau}H^{inc}_z) \end{aligned} \tag{28}$$

$$\begin{aligned} &-\frac{1}{\eta_0}[E_{\tau z}(J_z)+E_{\tau\tau}(J_\tau)+E_{\tau\tau}(M_\tau)]+\eta_{\tau z}[H_{\tau z}(J_z)+H_{\tau\tau}(J_\tau)+H_{\tau z}(M_z)+H_{\tau\tau}(M_\tau)]-\eta_{\tau\tau}[H_{z\tau}(J_\tau)+ \\ &H_{zz}(M_z)+H_{z\tau}(M_\tau)]=\frac{1}{\eta_0}(E^{inc}_\tau-\eta_{\tau z}H^{inc}_\tau+\eta_{\tau\tau}H^{inc}_z) \end{aligned} \tag{29}$$

where

$$\begin{aligned} E_{z\tau}(M_\tau) &= -\eta_{z\tau}H_{z\tau}(J_\tau)-\eta_{zz}H_{z\tau}(J_z) \\ E_{\tau z}(M_z) &= \eta_{\tau\tau}H_{\tau z}(J_\tau)+\eta_{\tau z}H_{\tau z}(J_z) \\ E_{\tau\tau}(M_\tau) &= -\eta_{z\tau}H_{\tau\tau}(J_\tau)-\eta_{zz}H_{\tau\tau}(J_z) \\ H_{zz}(M_z) &= -\eta_{\tau\tau}E_{zz}(J_\tau)-\eta_{\tau z}E_{zz}(J_z) \\ H_{z\tau}(M_\tau) &= \eta_{z\tau}E_{z\tau}(J_\tau)+\eta_{zz}E_{z\tau}(J_z) \\ H_{\tau z}(M_z) &= -\eta_{\tau\tau}E_{\tau z}(J_\tau)-\eta_{\tau z}E_{\tau z}(J_z) \\ H_{\tau\tau}(M_\tau) &= \eta_{z\tau}E_{\tau\tau}(J_\tau)+\eta_{zz}E_{\tau\tau}(J_z) \end{aligned} \tag{30}$$

Following the method of moments, the object contour C is divided into N linear segments with length ΔC^i as in [9], $i = 1, 2, \ldots, N$ and each current component is expanded into N unknown constant coefficients multiplied by the pulse basis function P^i. In an equation form, the unknown currents can be expressed as

$$J_{\begin{Bmatrix}z\\\tau\end{Bmatrix}}=\sum_i^N I^i_{\begin{Bmatrix}z\\\tau\end{Bmatrix}}P^i \tag{31}$$

where $I^i_{\begin{Bmatrix}z\\\tau\end{Bmatrix}}$ are the unknown current coefficients and $P^i = 1$ on the subdomain i and zero else where. Substituting (31) into the operators defined in the Appendix A and then substitute the operators in (28) and (29) and satisfy (28) and (29) at the match point (middle of the segments), the integral equation reduces to a matrix of order $2N$, which can be written in the form

$$\begin{aligned} &\{[Z]+[Y][\eta_s]+[\eta_f]([Y]+[Z][\eta_s])\}[I] \\ &\quad =[E]+[\eta_f][H] \end{aligned} \tag{32}$$

here the different matrices and column vectors are defined as in the following. The matrices [Z] and [Y] consist of four submatrices according to

$$[Z]=\begin{bmatrix} Z^{ij}_{zz} & Z^{ij}_{z\tau} \\ Z^{ij}_{\tau z} & Z^{ij}_{\tau\tau}\end{bmatrix} \quad and \quad [Y]=\begin{bmatrix} Y^{ij}_{zz} & Y^{ij}_{z\tau} \\ Y^{ij}_{\tau z} & Y^{ij}_{\tau\tau}\end{bmatrix} \tag{33}$$

The elements of the Z and Y matrices are given in Appendix B. The first suffix of the subscript refers to the field component and the second suffix refers to the electric current component. The superscript ij is the element order

in the submatrix; i for the matching field point in the middle of the segment i and j for the j's unit pulse. $[E]$ and $[H]$ are the excitation vectors due to the electric and magnetic fields, respectively defined by

$$[E] = \begin{bmatrix} E_z^{i\,inc} \\ E_\tau^{i\,inc} \end{bmatrix} \quad and \quad [H] = \begin{bmatrix} H_\tau^{i\,inc} \\ -H_z^{i\,inc} \end{bmatrix} \tag{34}$$

where i denotes the matching field point in the middle of the segment i. The expressions of these elements are given in Appendix B. The column vector containing the unknowns can be expressed as

$$[I] = \begin{bmatrix} I_z^j \\ I_\tau^j \end{bmatrix} \tag{35}$$

The matrices $[\eta_f]$ and $[\eta_s]$ each consists of four submatrices according to

$$[\eta_s] = \begin{bmatrix} \eta_{zz}^{ij} & \eta_{z\tau}^{ij} \\ \eta_{\tau z}^{ij} & \eta_{\tau\tau}^{ij} \end{bmatrix} \quad \text{and} \quad [\eta_f] = \begin{bmatrix} \eta_{\tau z}^{ij} & \eta_{\tau\tau}^{ij} \\ -\eta_{zz}^{ij} & -\eta_{z\tau}^{ij} \end{bmatrix} \tag{36}$$

where each submatrix is a diagonal matrix with $\eta_{\gamma\upsilon}^{ij}$ = the value of the surface impedance $\eta_{\gamma\upsilon}$ at the middle of the segment i when i = j and zero otherwise, where the subscripts γ and υ refer to z and τ. Once the matrices Z and Y are created and the excitation vectors $[E]$ and $[H]$ are filled and substituted in equation (32), the moment matrix system (32) can be solved to obtain the unknown current coefficients in (35).

4 DIFFERENT FORMULATIONS

In order to account for different formulations, one may use the E-field integral equation ($E_{tan} = 0$), or H-field integral equation ($\hat{u}_n \times H_{tan}) = 0$, both applied just inside the surface S with the equivalent currents defined in (15). Then combining them to obtain the combined field integral equations or use the IBC as an integral equation as described above. The moment matrix of these integral equations can be obtained if the matrix equation (32) is written in the following form

$$\begin{aligned} &\{\alpha([Z]+[Y][\eta_s])+\beta[\eta_f]([Y]+[Z][\eta_s])\}[I] \\ &\quad = \alpha[E]+\beta[\eta_f][H] \end{aligned} \tag{37}$$

where α and β are, respectively, the combination parameters weighing the electric field and the magnetic field just inside the surface S [2]. Thus different field formulations can be obtained by different selections of α and β. These formulations can be obtained according to Table I.

Table I
Generation of different formulations

Formulation type	α	β
IBCE	1.	0.
IBCH	0.	$-[\eta_f]^{-1}$
IBCC	1.	$-[\eta_f]^{-1}$
IBC	1.	1.

IBCE (IBCH) implies that the E-field (H-field) boundary condition is applied, i.e. the tangential electric (magnetic) field is assumed zero just inside the surface of the object, using the implementation of the IBC approximation for the magnetic current, i.e. the magnetic current is related to the electric current via the surface impedance as in Eqn (27). The third formulation IBCC denotes the combination of IBCE and IBCH on the impedance surface. The fourth formulation, IBC implies that the IBC is implemented explicitly on the equivalent currents and the tangential fields. The solutions from the IBCE and IBCH formulations are not unique where there are internal structure resonance frequencies. These cases can be treated by using the IBCC or IBC formulations. The solution of the IBC formulation is also not unique when the impedance is zero (perfect conducting case) or inductive. The problem of nonuniqueness will not be investigated in this paper. Interested readers may find this treated in [2] and [17].

5 SCATTERED FIELDS

Once any of the above formulations is solved the scattered field can be computed from the obtained electric current distribution. The field will be scattered along a cone of half angle $\theta = \pi - \theta_{inc}$ around the structure. In the cylindrical coordinate system it is sufficient to compute the z-components of the electric and magnetic fields in the far zone when r and ρ are much larger than the wavelength and the maximum cross sectional diameter of the object. This can be obtained, first, by using the large argument approxima-

tion of the Hankel functions in the field operators defined in Appendix A and also in their dual operators due to the magnetic currents, Second, neglect the high order terms of $1/\rho$. Third, substitute the magnetic current by the electric current and the surface impedance using (27). It can be found that in the cylindrical coordinate system, only z and ϕ components of the fields are contributing to the far field. The spherical components of the electric field E_θ and E_ϕ, which are more appropriate to use in the oblique incidence case, can be obtained from the cylindrical field components E_z and H_z, respectively. Therefore, by using simple transformations the spherical electric field components can be written as

$$E_\phi^{sc}(\theta,\phi) = \eta \sqrt{\frac{j}{8\pi k_\rho \rho}}\, e^{-j(k_\rho \rho - k_z z)} \sum_{i=1}^{N} \Delta C^i\, e^{jk_\rho (\hat{u}_\rho \cdot \rho_i)} \times I_{\tau_i} [\, k_\rho\, \eta_{\tau\tau} - k_0\, (\hat{u}_\rho \cdot \hat{u}_{n_i}) - k_z\, \eta_{z\tau}\, (\hat{u}_\rho \cdot \hat{u}_{\tau_i})] + I_{z_i} [k_\rho\, \eta_{\tau z} - k_z\, \eta_{zz}\, (\hat{u}_\rho \cdot \hat{u}_{\tau_i})] \tag{38}$$

$$E_\theta^{sc}(\theta,\phi) = \sqrt{\frac{j}{8\pi k_\rho \rho}}\, e^{-j(k_\rho \rho - k_z z)} \sum_{i=1}^{N} \Delta C^i e^{jk_\rho (\hat{u}_\rho \cdot \rho_i)} \times I_{z_i} [k_0 (\hat{u}_\rho \cdot \hat{u}_{n_i}) \eta_{zz} - k_\rho] + I_{\tau_i} [k_0\, (\hat{u}_\rho \cdot \hat{u}_{n_i})\, \eta_{z\tau} - k_z\, (\hat{u}_\rho \cdot \hat{u}_{\tau_i})] \tag{39}$$

In this paper the scattered fields are computed and normalized to $\sqrt{2j/\pi k_\rho \rho}$.

6 RESULTS

First, to verify the code, a circular cylinder with an arbitrary anisotropic impedance is considered. The parameters are ka=3.0, with arbitrary surface impedance of η_{zz}= 0.5+j0.1, $\eta_{z\tau}$=0.3+j0.6, $\eta_{\tau z}$=0.3+j0.5 and $\eta_{\tau\tau}$=0.7-j0.3 (these values are chosen arbitrarily) and the plane wave parameters are θ_{inc}=45°, ϕ_{inc}=180°, and α_{inc}=45°. The surface electric current components are plotted in Fig. 2a (against the exact solution obtained from the series solution in [14]), ten and twenty segments per wavelength are used in the numerical solution based on the IBC formulation. Acceptable results are obtained with 10 segments per wavelength and more accurate results are obtained when 20 segments are used. Also the scattered far fields are computed and plotted in Fig. 2b and compared with the exact solutions. It is obvious that the solution using 20 segments per wavelength gives more accurate results within the whole ϕ-range. Notice that neither the fields nor the currents distribution are symmetric around the plane of incidence because the incident wave is chosen to have both TE_z and TM_z incident polarizations simultaneously and also because of the unequality of the surface impedances values $\eta_{z\tau}$ and $\eta_{\tau z}$.

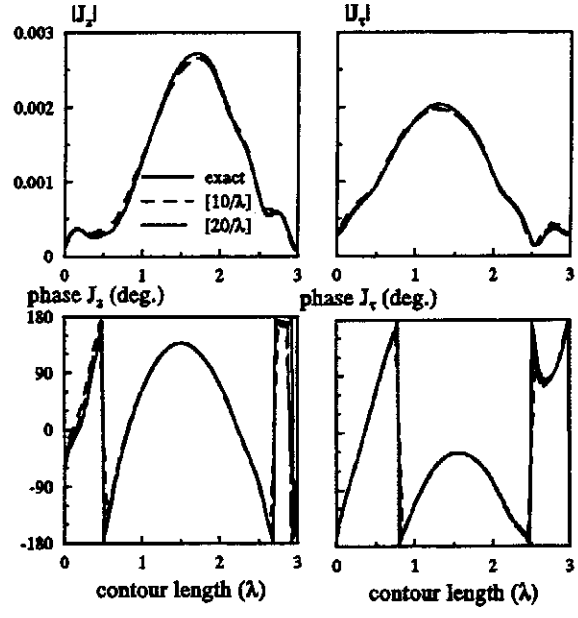

Fig. 2a Exact and numerical current distribution on a circular cylinder with, ka=3.0, η_{zz}=0.5+j.1, $\eta_{z\tau}$=0.3+j.6, $\eta_{\tau z}$=0.3 +j.5 and $\eta_{\tau\tau}$=0.7-j.3, illuminated by a plane wave with θ_i=45°, ϕ_i = 180°, and α_i = 45°.

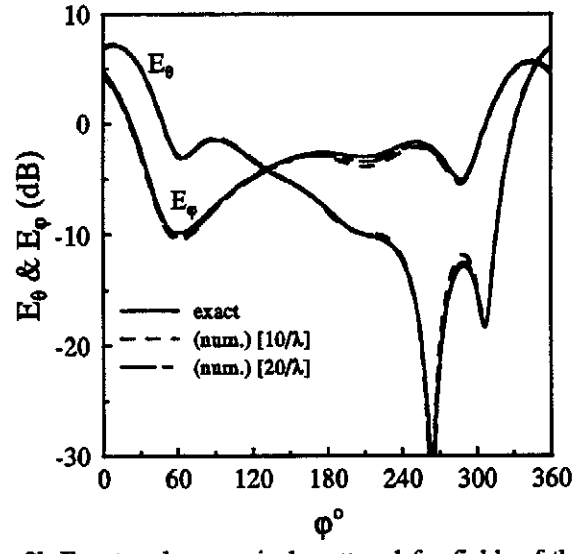

Fig. 2b Exact and numerical scattered far fields of the example in Fig. 2a.

Now we consider some practical configurations. The first example is again a circular cylinder, but now with η_{zz} = - j50.0, $\eta_{zT} = \eta_{Tz} = \eta_{TT} = 0.0$, θ_{inc}=45°, ϕ_{inc} = 180°, and α_{inc} = 45°. This surface impedance represents transverse corrugations. The actual corrugated surface is very difficult to analyze [18]. The impedance model is much simpler and easier to analyze and an exact solution can be found as considered in [14]. The exact solution is compared with the present moment method solution using the IBC formulation with 20 segment per wavelength. The current distributions are plotted in Fig. 3a. Very good agreement can be noticed between both solutions. Also, one must notice that the current component J_z normal to the corrugations is almost zero. This is expected as J must flow entirely along the corrugations. This is a good verification that the surface impedance considered in this example is a good approximation of the transverse corrugated cylinder. The scattered far fields are given in Fig. 3b. The exact and the numerical solutions are indistinguishable. Notice also, the skew symmetry between E_θ and E_ϕ components which is also expected for oblique incidence and 45 degree polarization. For normal incidence E_θ and E_ϕ could be equal for all ϕ for 45 degree incident polarization if the impedance $\eta_{zz} = \infty$.

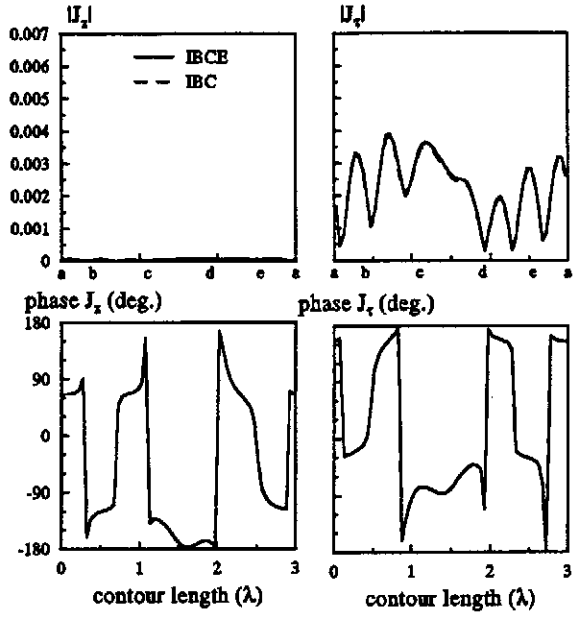

Fig. 3a Exact and numerical current distribution on a circular cylinder with, ka=3.0, and η_{zz}=-j50., $\eta_{zT}=\eta_{Tz}$ $=\eta_{TT}=0.0$, illuminated by a plane wave with θ_{inc}=45°, ϕ_{inc} = 180°, and α_{inc}= 45°.

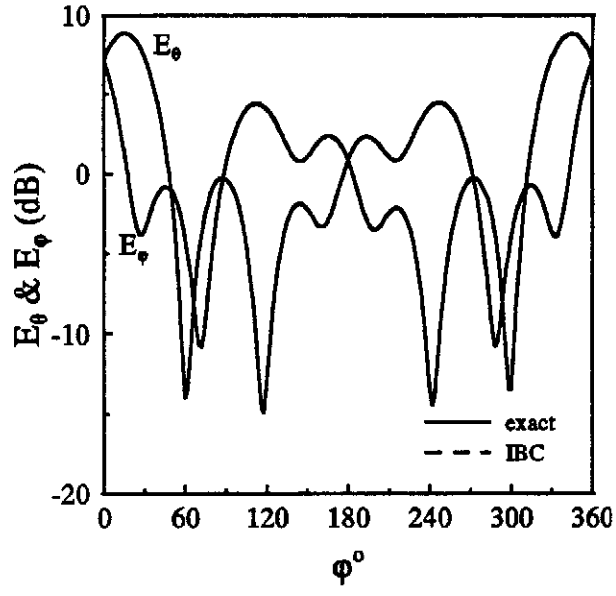

Fig. 3b Exact and numerical scattered far fields of the example in Fig. 3a.

An impedance cylinder with square cross-section is considered as shown in Fig. 4a. This geometry has no analytic solution. The surface impedance is used to model soft corrugated surfaces. The corrugations of the sides A and C are considered to be along the transverse direction parallel to the xy-plane with an equivalent surface impedance assumed to be η_{zz}=-j50.0, η_{zT}= η_{Tz}= η_{TT}=0.0. The

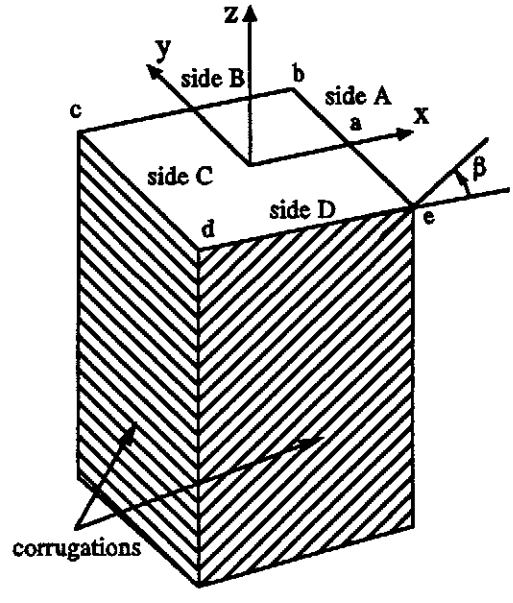

Fig. 4a Geometry of a corrugated square cylinder.

corrugations on the sides B and D are assumed to be of the same parameters as that on sides A and C (i.e. has the same surface impedance with respect to the coordinates of the corrugations with $\eta_{\zeta\zeta}$=-j50.0, $\eta_{\zeta\xi}=\eta_{\xi\zeta}=\eta_{\xi\xi}=0.$), but tilted by an angle $\beta=45^\circ$ with the x-axis. The equivalent surface impedance with respect to the object surface coordinates using (8) is given as $\eta_{zz}=\eta_{zT}=\eta_{Tz}=\eta_{TT}$ = -j25.0 on the side D and $\eta_{zz}=\eta_{TT}$ = -j25.0, $\eta_{zT}=\eta_{Tz}$ = +j25.0 on the side B. The electric surface current components and the scattered far fields are computed due to a plane wave with $\theta_i=45^\circ$, $\alpha_i = 0^\circ$ (TM_z polarization) and $\phi_i = 180^\circ$. The current distributions are plotted in Fig. 4b from the IBCE and IBC formulations. Notice that the x-axis of the upper two figures (current magnitude) are indicated by the letters a, b, c, d, e, and a which are corresponding to the surface positions given in Fig. 4a. In the lower two figures (current phase) the x-axis is indicated by the contour length starting from the point a on Fig. 4a. The scattered far fields are plotted in Fig. 4c. In these figures the solution from the IBCE and IBC formulations are presented and compared against each other. It can be noticed that the solutions obtained from both formulations are in good agreement with each other. It is clear that the scattered fields are symmetric around the xz-plane (plane of incidence) when $\phi_i = 180^\circ$ because of the object symmetry around this plane and because of the pure TM_z polarization of the wave incident. The ϕ-component of the scattered field is zero along the plane of incidence in the forward and the back scattered directions because of the skew symmetry of the J_τ component which is obvious from the phase distribution of the current. When the incident wave is TE_z polarized, the current distributions and the scattered far fields are given in Figs. 5a and 5b, respectively. One should notice that the scattered E-field E_θ and E_ϕ for TM_z polarization of the incident wave is nearly equal to the E_ϕ and E_θ, respectively for TE_z polarization of the incident wave. This corresponds to E-field for TM_z polarization being equal to H-field for TE_z polarization, which is expected as the cylinder is close to soft (it would have been ideally soft if $\eta_{\zeta\zeta}=\infty$) and therefore has polarization independent scattering characteristics according to [7]. The electric current component normal to the corrugations must be zero. To check this for our example the electric current components along and normal to the corrugations are computed from the currents in Fig. 4b and 5a and plotted in Figs. 6a and 6b, respectively. One should notice that the current components normal to the corrugations are nearly zero for both TM_z and TE_z incidence as expected. This can also be considered as a verification of the code.

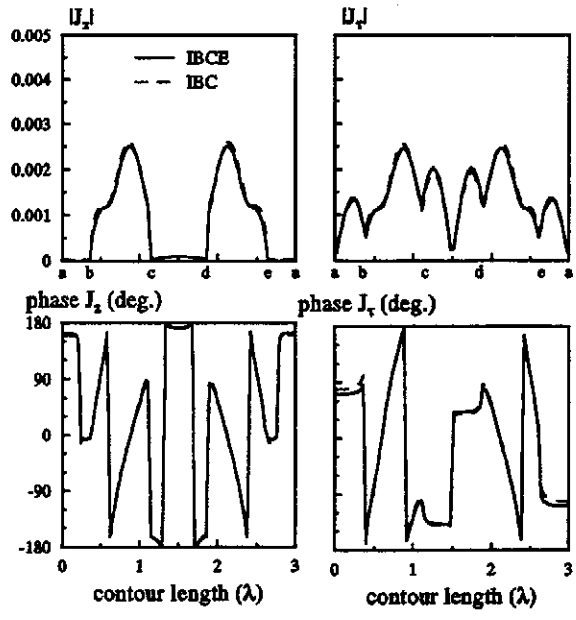

Fig. 4b Electric current distribution of the geometry in Fig. 4a with, η_{zz} = - j50.0, $\eta_{zT}=\eta_{Tz}=\eta_{TT}$ = 0.0 on side A and C, $\eta_{zz}=\eta_{zT}=\eta_{Tz}=\eta_{TT}$ = -j25.0 on the side D and $\eta_{zz}=\eta_{TT}$ = - j25.0, $\eta_{zT}=\eta_{Tz}$ = +j25.0 on the side B. The cylinder side length = 0.75 λ. The plane wave with $\theta_{inc}=45^\circ$, $\alpha_{inc} = 0^\circ$, and $\phi_{inc} = 180^\circ$.

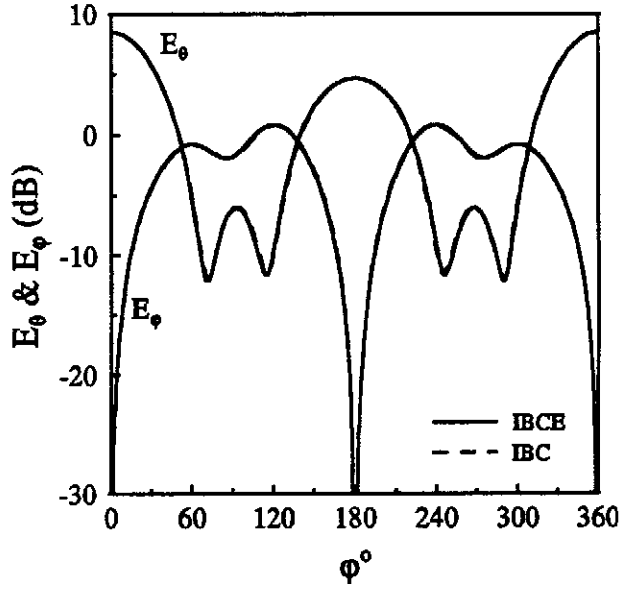

Fig. 4c, numerical scattered far filed of the object in Fig. 4a with the parameters in Fig. 4b.

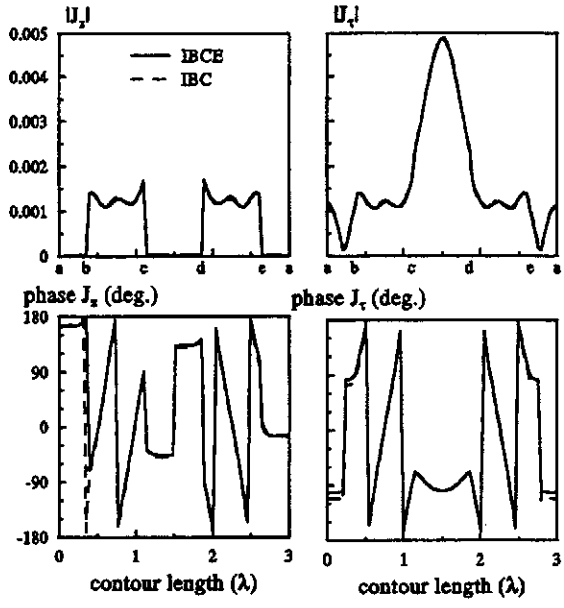

Fig. 5a Electric current distribution of the geometry in Fig. 4a with the same parameters in Fig. 4a and the plane wave with $\theta_{inc}=45^o$, $\alpha_{inc} = 90^o$, and $\phi_{inc} = 180^o$.

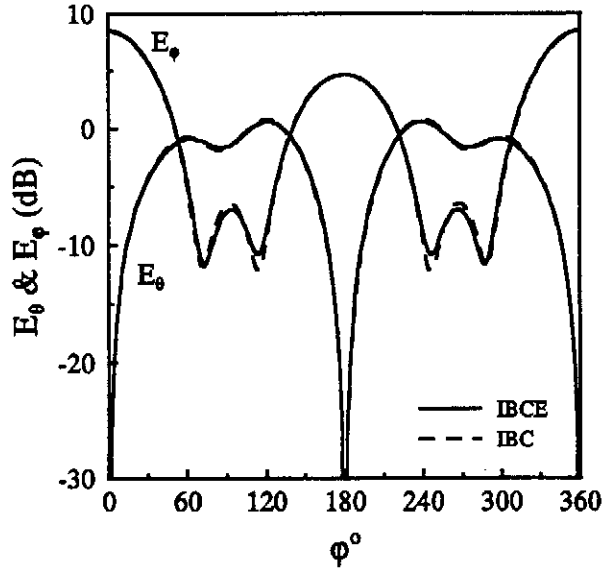

Fig. 5b, numerical scattered far filed of the object in Fig. 4a with the parameters in Fig. 5a.

7 CONCLUSIONS

The integral equation for the problem of electromagnetic scattering from arbitrary 2D objects with anisotropic surface impedance due to obliquely incident plane wave with arbitrary linear polarization is derived. The surface impedance is anisotropic with an arbitrary principal direction. The integral equations are solved by the method of moments with pulse basis functions and point matching. Four different surface integral equations are actually implemented. In the numerical evaluation of the matrix elements four point Gaussian quadrature is used. It is also found that 10 basis functions per wavelength gives reasonable results, but 20 segments per wave length is enough for most applications to obtain accurate results in the near and far fields. For objects with large cross sections in terms of wavelength more segments may be needed in order to get full convergence in weak field regions or in regions of rapidly varying currents. The numerical solutions are verified against the analytical solutions of circular cylinders. A theoretical example is constructed for which the E-field solution for TM_z incidence should be equal to the H-field solution for TE_z incidence. The example is a cylinder with square cross section with soft surfaces, such as corrugations that are tilted to become normal to the k vector for the given oblique incidence. The results are found to behave as expected. This example illustrates the significance of the present solution in order to simplify complex structures that may be very difficult to solve using other models.

The IBC is valid for perfectly electric conducting surfaces where the surface impedance is zero as well as to all

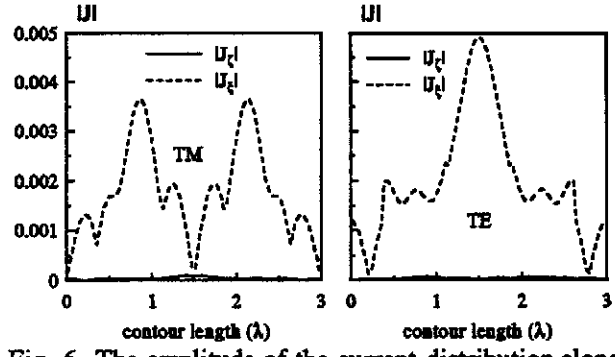

Fig. 6. The amplitude of the current distribution along and normal to the corrugation in Fig. 4a. (a) for the case in Fig. 4b and (b) for the case in Fig. 5a.

surfaces of finite surface impedances. If the impedance is infinite (perfect magnetic conductor) one must use another formulation based on the surface admittance which can be obtained from applying duality on (1) (not presented here). We may refer to this boundary condition as the admittance boundary condition (ABC). Therefore, it is expected that the numerical accuracy will deteriorate when the surface impedance values are much larger than the values used in this paper. To improve that one may use the ABC formulation, which is expected to be more accurate in such cases. This subject and this formulation will be considered in a future study with some discussions on the accuracy and limitations on these formulations.

8 REFERENCES

[1] T. B. A. Senior, "Approximate boundary conditions," *IEEE Trans. Antennas Propagat.*, vol. 29, pp. 826-829, 1981.

[2] A. A. Kishk,"Electromagnetic scattering from composite objects using a mixture of exact and impedance boundary conditions," *IEEE Trans. Antennas Propagat.*., vol. AP-39, pp. 826-833, 1991.

[3] J. R. Wait, "Use and misuse of impedance boundary conditions in electromagnetics", *Proc. PIERS Symposium*, Boston, MA, p. 358, July 1989.

[4] T. B. A. Senior and J. L. Volakis,"Derivation and application of a class of generalized boundary conditions," *IEEE Trans. Antennas Propagat.*, vol. AP-37, pp. 1566-1572, 1989.

[5] D. J. Hoppe and Y. Rahmat-Sami,"Scattering by superquadric dielectric-coated cylinders using higher order impedance boundary conditions," *IEEE Trans. Antennas Propagat.*, vol. 40, pp. 1513-1523, 1992.

[6] K. A. Iskander, L. Shafai, A. Frandsen, and J. E. Hansen, "Application of impedance boundary conditions to numerical solution of currugated circular horns, *IEEE Trans. Antennas Propagat.*, vol. 30, pp. 366-372, 1982.

[7] P.-S. Kildal,"Artificially soft and hard surfaces in electromagnetics," *IEEE Trans. Antennas Propagat.*, vol. 38, pp. 1537-1544, 1990.

[8] P.-S. Kildal, A. A. Kishk, and A. Tengs, "Reduction of forward scattering from cylindrical objects using hard surfaces," submitted to *IEEE Trans. Antennas Propagat.*, April 1995.

[9] P. M. Goggans, "A combined method-of-moments and approximate boundary condition solution for scattering from a conducting body with a dielectric-filled cavity," *Ph.D. Dissertation*, Auburn University, 1990.

[10] A. A. Kishk, and P. M. Goggans,"Electromagnetic scattering from two-dimensional composite objects," *ACES Journal*, vol. 9, no. 1, pp.32-39, 1994.

[11] Gordon, R., and A. A. Kishk,"An efficient finite element method for determining the scattering from lossy cylinders using the impedance boundary condition and an absorbing boundary condition due to oblique incident," *9th Annual Review of Progress in Applied Comput.. Electromagnetics, Conf. Proc.*, pp. 871-878, 1993.

[12] Yan, Jun, R.K. Richard, and A. A. Kishk, Electromagnetic scattering from impedance elliptic cylinders using finite deference method (oblique incidence), *Journal of Electromagnetics*, vol. 15, pp. 157-173, 1995.

[13] A. W. Glisson, M. Orman, and D. Koppel, "Electromagnetic scattering by a body of revolution with a general anisotropic impedance boundary condition," *IEEE Antennas Propagat. Soc. Int. Symp. Dig.*, vol. 4, pp. 1997-2000., June 1992.

[14] A. A. Kishk, and P.-S. Kildal,"Electromagnetic scattering from a circular cylinder with an anisotropic surface impedance due to an obliquely incident plane wave," *Microwave and Optical Technology Letters*, vol. 10, no. 3, 1995.

[15] P.-S. Kildal, S. Rengarajan, and A. Moldsvor, Analysis of nearly cylindrical antennas and scattering problems using a spectrum of two-dimensional solutions," submitted to *IEEE Trans. Antennas Propagat.*, April 1995.

[16] R. F. Harringtopn, *Time-Harmonic Electromagnetic fields*, McGraw-Hill Book Company, 1961.

[17] J. M. Putnam and L. N. Medgyesi-Mitschang,-"Combined field integral equation formulation for inhomogeneous two- and three-dimensional bodies: The junction problem," *IEEE Trans. Antennas Propagat.*, vol. AP-39, pp. 667-672, No. 5, 1991.

[18] G. Manara, G. Pelosi, A. Monorchio, and R. Coccioli,"Plane-wave scattering from cylinders with transverse corrugations," *Electronics Letters*, vol. 31, pp. 437-438, 1995.

APPENDIX A

Electric and magnetic field operators due to the electric current components are expressed as

$$E_{zz}(J_z) = -\frac{k_\rho^2}{4\omega\epsilon_0}\int_C J_z\, H_0^{(2)}(k_\rho\Delta\rho)dl' \tag{A-1}$$

$$E_{\tau z}(J_z) = \frac{-jk_\rho k_z}{4\omega\epsilon_0}\int_C J_z H_1^{(2)}(k_\rho\Delta\rho)(\hat{u}_\tau \cdot \Delta\hat{\rho})dl' \tag{A-2}$$

$$E_{z\tau}(J_\tau) = \frac{-jk_z k_\rho}{4\omega\epsilon_0}\int_C J_\tau H_1^{(2)}(k_\rho\Delta\rho)(\hat{u}_\tau{}' \cdot \Delta\hat{\rho})dl' \tag{A-3}$$

$$\begin{aligned} E_{\tau\tau}(J_\tau) = -\frac{1}{4\omega\epsilon_0}\int_C & k^2 J_\tau\{(\hat{u}_\tau{}' \cdot \hat{u}_\tau)H_0^{(2)}(k_\rho\Delta\rho) \\ & -\frac{k_\rho}{\Delta\rho}H_1^{(2)}(k_\rho\Delta\rho)(\hat{u}_\tau{}' \cdot \hat{u}_\tau) - k_\rho[k_\rho H_0^{(2)}(k_\rho\Delta\rho) \\ & -\frac{2}{\Delta\rho}H_1^{(2)}(k_\rho\Delta\rho)](\hat{u}_\tau{}' \cdot \Delta\hat{\rho})(\hat{u}_\tau \cdot \Delta\hat{\rho})\}dl' \end{aligned} \tag{A-4}$$

$$H_{zz}(J_z) = 0 \tag{A-5}$$

$$H_{\tau z}(J_z) = -\frac{1}{4}\int_C J_z H_1^{(2)}(k_\rho\Delta\rho)(\hat{u}_n \cdot \Delta\hat{\rho})dl' \tag{A-6}$$

$$H_{z\tau}(J_\tau) = -\frac{k_\rho}{4j}\int_C J_\tau H_1^{(2)}(k_\rho\Delta\rho)(\hat{u}_n{}' \cdot \Delta\hat{\rho})dl' \tag{A-7}$$

$$H_{\tau\tau}(J_\tau) = -\frac{k_z}{4}\int_c J_\tau\, H_0^{(2)}(k_\rho\Delta\rho)\,(\hat{u}_\tau \cdot \hat{u}_n{}')\,dl' \tag{A-8}$$